Diagnostic Imaging

PET-CT and PET-MRI in Oncology

A Practical Guide

Bearbeitet von
Patrick Peller, Rathan Subramaniam, Ali Guermazi

1. Auflage 2012. Buch. xvii, 435 S. Hardcover
ISBN 978 3 642 01138 2
Format (B x L): 19,3 x 26 cm
Gewicht: 1043 g

Weitere Fachgebiete > Medizin > Sonstige Medizinische Fachgebiete > Kernspintomographie (CT, NMR, MRT, etc.)

Zu Inhaltsverzeichnis

schnell und portofrei erhältlich bei

beck-shop.de
DIE FACHBUCHHANDLUNG

Die Online-Fachbuchhandlung beck-shop.de ist spezialisiert auf Fachbücher, insbesondere Recht, Steuern und Wirtschaft. Im Sortiment finden Sie alle Medien (Bücher, Zeitschriften, CDs, eBooks, etc.) aller Verlage. Ergänzt wird das Programm durch Services wie Neuerscheinungsdienst oder Zusammenstellungen von Büchern zu Sonderpreisen. Der Shop führt mehr als 8 Millionen Produkte.

PET Radiochemistry and Radiopharmacy

Mark S. Jacobson, Raymond A. Steichen, and Patrick J. Peller

Contents

Abstract

The vast majority of PET radiopharmaceuticals today are cyclotron produced. Carbon-11 (^{11}C), Nitrogen-13 (^{13}N), Oxygen-15 (^{15}O) products are created for in-house use only due to their short half-lives. The longer half-life of Fluorine-18 means that ^{18}F-labeled PET radiotracers can be widely distributed. Production of radiopharmaceuticals is computer-controlled and automated. Automation increases both reliability and efficiency of PET operations while decreasing the radiation dose to the staff. For today, FDG remains the workhorse of oncologic PET imaging. Additional ^{18}F PET radiotracers directed at a range of molecular processes are being studied and should become available in the future.

1 Introduction

Positron emission tomography (PET) has become a powerful research and clinical imaging tool for evaluating complex biochemical processes in cancer patients. PET has developed rapidly as radiochemistry and radiopharmacy have advanced. The oncologic clinical applications of PET have increased dramatically over the past decade because of the synthesis and widespread distribution of one molecule, ^{18}Fluorine-2-Fluoro-2-Deoxy-glucose (FDG). FDG PET/CT has become essential in evaluating cancer patients in major medical centers throughout the world. Measurement of normal and altered biochemical pathways noninvasively is routinely performed with PET radiopharmaceuticals. The continued

M. S. Jacobson (✉) · P. J. Peller
Department of Radiology, Mayo Clinic,
200 1st Street SW, Rochester, MN 55905, USA
e-mail: jacobson.mark17@mayo.edu

R. A. Steichen
Section of Equipment Services, Mayo Clinic,
200 1st Street SW, Rochester, MN 55905, USA

P. Peller et al. (eds.), *PET-CT and PET-MRI in Oncology*, Medical Radiology. Diagnostic Imaging,
DOI: 10.1007/174_2012_703, © Springer-Verlag Berlin Heidelberg 2012

Table 1 PET radionuclides

Radionuclide	Half-life (min)
Carbon-11	20.4
Nitrogen-13	9.98
Oxygen-15	2.03
Fluorine-18	109.8
Copper-62	9.74
Gallium-68	68.3
Rubidium-82	1.25
Iodine-122	3.62
Iodine-124	6019.2

growth of PET will require the expansion of clinically available positron emitting radiopharmaceuticals (Vallabhajosula et al. 2011, Rice et al. 2011).

2 Positron Emitting Radionuclides

Of the more than 3,000 known neutron and proton configurations, approximately 250 are stable and more than 2,500 are radioactive. The majority of the radioactive nuclides are artificially produced in cyclotrons or reactors. Of these radioactive nuclides, ten are major positron emitters (Table 1). PET imaging makes use of these positron-emitting radionuclides for clinical and research applications (McCarthy and Welch 1998). There are three primary methods to produce radioactive atoms for nuclear imaging. Radioisotopes are either reactor produced from fission by-products by chemical separation, or by neutron irradiation of a specific target; or they are produced in a cyclotron from bombardment of a target material with charged particles.

2.1 Cyclotron Produced

Carbon-11 (^{11}C), Nitrogen-13 (^{13}N), Oxygen-15 (^{15}O) and Fluorine-18 (^{18}F) are low-molecular-weight radioisotopes produced in a cyclotron. One of the great advantages of positron emission tomography is the use of positron emitting radioisotopes that can be easily added to biomolecules, especially ^{11}C, ^{13}N, ^{15}O and ^{18}F. All 4 also possess simple decay schemes with each emitting a single positron. Substituting ^{11}C, ^{13}N and ^{15}O for stable ^{12}C, ^{14}N and ^{16}O does not alter the function or configuration of the compound. ^{18}F often replaces a hydroxyl group, which only mildly affects the biologic behavior of the molecule.

The disadvantage of ^{11}C, ^{13}N and ^{15}O labeled compounds is that their half-life is very short. The 2-minute half-life of ^{15}O requires a tube direct from the cyclotron and pumping the ^{15}O labeled compounds immediately into the scan room. The complicated chemistry of ^{13}N and its 10-min half-life leaves too little time for radiopharmaceutical synthesis and imaging. ^{11}C with its 20-min half-life has labeled a vast array of biological radiotracers in the research realm to measure molecular kinetics and function. ^{11}C radiopharmaceuticals require rapid synthesis and scanning, which make an on-site cyclotron mandatory. Only ^{18}F with its nearly 2-h half-life allows time for complex syntheses or delayed imaging and it can be transported significant distances (Schlyer 2004).

2.1.1 Cyclotron

A medical cyclotron (Fig. 1) is a particle accelerator that can produce PET radionuclides. It is composed of two flat D-shaped hollow metal electrodes in the vacuum chamber between the two poles of a large electromagnet. In the center hydrogen (H_2) or deuterium (D_2) gas is introduced to yield the particles to be accelerated (H^- or D^-). Under the effect of a strong magnetic field, these anions gain energy from high-frequency alternating voltage applied between the electrodes. The magnetic field and the increasing energy of the particles force the anions to travel in a spiral path. The radius of the anion's path increases until the particles hit a stripping foil at the perimeter of the vacuum chamber. The stripping foil removes the electrons from the anions forming positively charged particles, H^+ or D^+. The change in charge deflects the particles out of the acceleration chamber to collide with the contents of the target. The high-energy particle smashes into a stable isotope target, yielding positron-emitting radionuclides (Shaiju et al. 2009).

2.1.2 Cyclotron Created Radionuclides

The synthesis of positron emitting biomolecules begins from small precursor compounds that are generated from a cyclotron target. There a limited number of small precursors that can originate in a cyclotron. The energy of the particle and density of the beam particle as well as the nuclear reaction determines the quantity

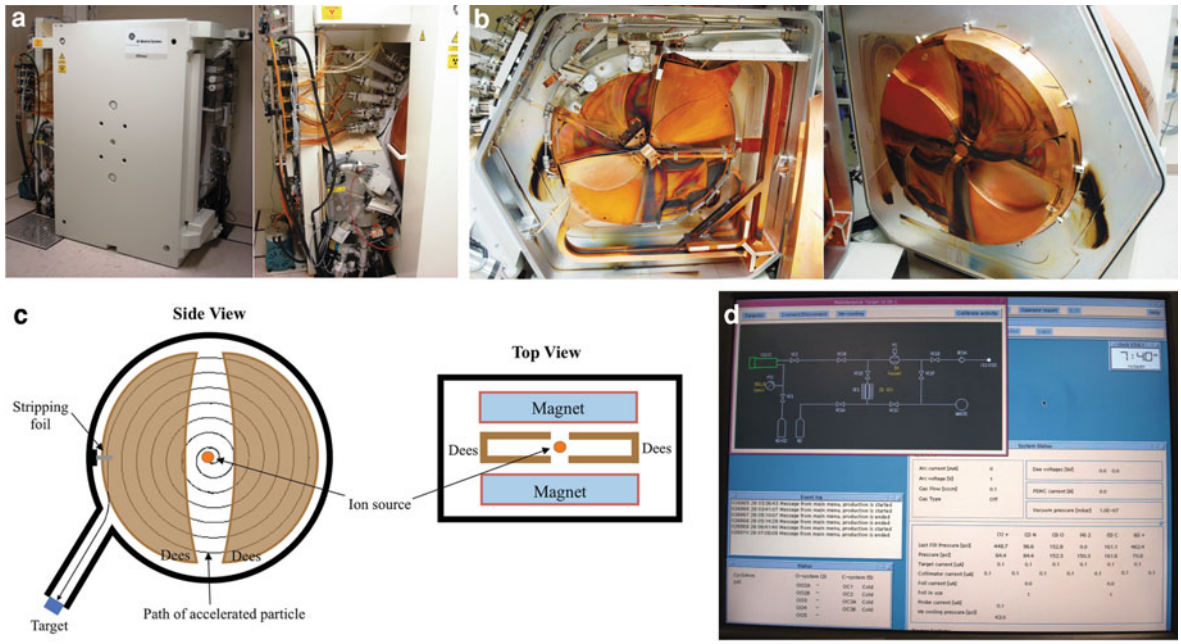

Fig. 1 This is the outside (**a**) and inside (**b**) of an upright PET cyclotron with dual particle capability. Six target ports on the left side of the cyclotron can be used for dual target irradiation. The cyclotron (**c**) contains two major parts: a large electromagnet and two semicircular, hollow electrodes called "dees" because of their D-shape. The ions are injected into the center of the cyclotron and come under the affect of the alternating current applied to the dees and the magnetic field supplied by the electromagnet. The current is carefully timed so that the polarization of the dees changes as the particles dart from side to side. This accelerates the ions propelling them in a spiral faster and faster. At the maximum radius of the spiral, the ions hit the stripping foil and exit the cyclotron. The charged particles exiting the cyclotron impact the target to produce PET radionuclides. The cyclotron is computer controlled (**d**), allowing easy and efficient production of PET radiopharmaceuticals

and type of radionuclide produced. The specific activity of the radionuclide produced is equal to the activity per unit of material, often given in terms of the activity per gram. The radionuclide purity is the percentage of the radioactive species that is the desired isotope (Sharma et al. 2006).

Four major positron emitters are produced within a medical cyclotron: Carbon-11 (^{11}C), Nitrogen-13 (^{13}N), Oxygen-15 (^{15}O) and Fluorine-18 (^{18}F). ^{11}C is produced by proton bombardment of natural nitrogen. The proton interacts with stable ^{14}N and produces a neutron and ^{11}C. The target typically contains 2 % oxygen in the nitrogen and yields ^{11}C-carbon dioxide. ^{13}N is produced by proton bombardment of distilled water. The proton interacts with stable ^{16}O and produces an alpha particle and ^{13}N. ^{15}O is produced by deuteron bombardment of natural nitrogen. The deuteron interacts with stable ^{14}N and produces ^{15}O. Oxygen-15 is produced as either ^{15}O-molecular oxygen, ^{15}O-water or ^{15}O-carbon dioxide. Fluorine-18 (^{18}F) is produced by proton bombardment of Oxygen-18 enriched water. The proton interacts with the ^{18}O and produces a neutron and ^{18}F (Schlyer 2004).

2.2 Generator Derived Radionuclides

The Molybdenum-99/Technetium-99m generator is the major source for radionuclides in general nuclear medicine practice. The Tc-99m used to label a wide variety of compounds is eluted from the molybdenum-99 generator. Similar generator systems exist for positron emitting radionuclides (Table 2). Radionuclide generator systems consist of a parent radionuclide, which is a relatively long-lived radionuclide that decays into a much shorter-lived and chemically different daughter radionuclide. The system typically has the parent nuclide in a column from which the daughter is eluted when needed. The advantage of generator-produced positron emitting radionuclides is

Table 2 Generator produced positron emitting radionuclides

Parent	Daughter
Strontium-82 (half-life 25 days)	Rubidium-82 (half-life 1.25 min)
Germanium-68 (half-life 275 days)	Gallium-68 (half-life 68.3 min)
Zinc-62 (half-life 9.13 h)	Copper-62 (half-life 9.74 min)

the increased availability of short-lived radionuclides without an on-site cyclotron (Breeman and Verbruggen 2007; Williams et al. 2005; Zhernosekov et al. 2007; Zweit et al. 1992). The Rubidium-82 from a Strontium-82 generator is FDA approved for myocardial perfusion imaging. Gallium-68 and Copper-62 are not available for clinical use in the US. These metal radionuclides can label peptides and proteins coupled by a chelating agent. A number of ^{68}Ga-somatostatin analogs are being studied for tumor imaging (Rufini et al. 2007).

3 PET Radiotracer Production

3.1 Synthesis

Within the radiochemistry lab, quality assurance and quality control are of paramount importance. Quality control includes chemical and radiochemical purity determination and radiopharmaceutical validation. Time dominates all aspects of a PET study, particularly in the production of PET radionuclides. PET tracers must be synthesized and imaged rapidly taking into account the half-life of the radioisotope. For Carbon-11 labeled tracers with a 20-min half-life, this typically means 10 min for isotope production, 40 min for synthesis and 60–90 min for PET imaging. Since radiotracers are typically administered intravenously, procedures must be developed to produce high yield radiotracers that are chemically, radiochemically and biologically pure (Schlyer 2004).

3.2 Quality Control

Each radiolabeling procedure is validated by testing batches for sterility, presence of endotoxins, heavy metal contamination, pH, chemical purity, radionuclide identification, and radionuclide purity. Since time is vital for a PET radiopharmaceuticals, only initial validation is performed prior to release of the radiopharmaceutical. Subsequent testing on each batch ensures the continued safety of the manufacturing process. PET radiopharmaceutical testing is often automated with thin layer chromatography, high performance liquid chromatography or gas chromatography (Sharma et al. 2006).

3.3 Automated Production

Routine production of PET radiopharmaceuticals is computer controlled and automated. These automated synthesis units allow regular production of PET tracers with speed and efficiency, but without significant radiation exposure to laboratory personnel. These modules allow a series of reactions to occur under computer control. The operator guides the computer software to perform the complex synthetic procedures required to make PET tracers. Automated synthesis units can produce different radiotracers with the same or similar equipment. Indeed, the modular approach has been extended to the point that sterile disposable cartridges are now available to produce pure and pyrogen-free PET radiotracers for clinical use. High-yield production of FDG has been validated and cartridges for other PET radiopharmaceuticals are now available (Gatley 2003; Schlyer 2004).

3.4 Dispensing

Originally, PET radiopharmaceuticals were dispensed and administered as unit doses by hand. As with so much else in busy PET practices, FDG dosing is now automated. An FDG-filled tungsten-shielded multidose vial is placed inside the shielded cart and each dose is automatically measured and calibrated (Fig. 2). The FDG dose measured by an ionization chamber is automatically delivered directly to the patient. An easy-to-use touch screen initiates the injection and clearly shows prescribed and actual activity. The touch screen interface controls delivery of a specific dose for each patient that is consistently within 2 % of the prescribed dose. The equipment cart is mobile allowing easy movement to patient location. By eliminating manual unit dose preparation and

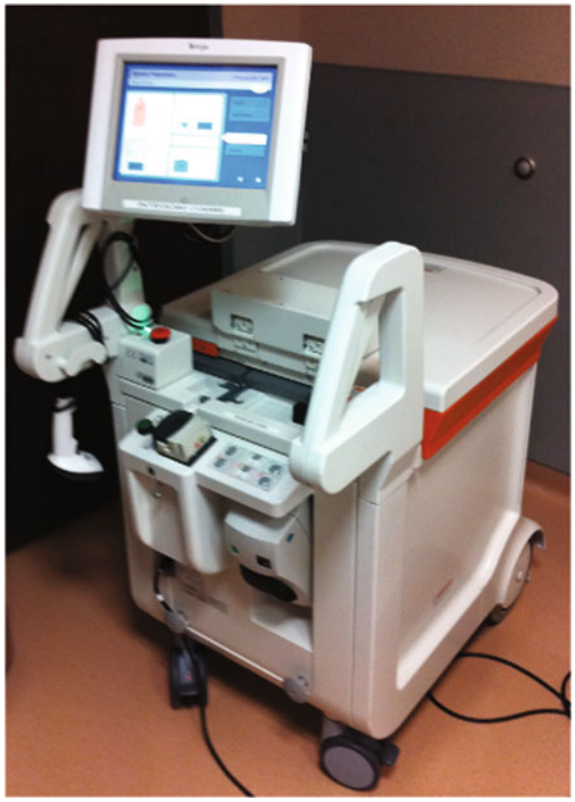

Fig. 2 This is an example of a mobile FDG administration device. From the shielded multidose vial within the machine, the individual patient's FDG activity is measured and administered. FDG dosing is controlled via computer to provide efficient delivery consistently within 2 % of the requested amount

injection, radiation exposure to both radiopharmacy and imaging personnel decreases more than 20 % (Carolan et al. 2012).

4 Oncologic PET Radiopharmaceuticals

In the last 30 years, several thousand PET radiotracers for oncologic imaging have been developed in more than 600 PET radiopharmacies worldwide. Despite the availability of so many PET radiopharmaceuticals for oncologic imaging, FDG remains the primary agent. Approximately 95 % of all PET studies for patients with cancer are performed with FDG.

4.1 FDA Approved

4.1.1 ^{18}F-2-Fluoro-2-Deoxy-Glucose

Warburg first reported increased glucose consumption by cancer cells compared to normal cells (Warburg 1956). In 1960 2-Deoxy-D-glucose was developed as a chemotherapeutic agent but it blocked glucose use by both normal and cancer cells (Laszlo et al. 1960). In 1976, ^{18}F-2-fluoro-2-deoxy-glucose (FDG) was first synthesized at Brookhaven National Laboratory (Ido et al. 1978; Pacák and Cerny 2002) (Fig. 3). Initially FDG PET was used to image cerebral glucose metabolism. Oncologic imaging began with brain tumors in part because of the small aperture in the early PET scanners. FDG was investigated in animal models with a wide range of malignancies. Clinical oncologic imaging was limited to the brain until PET body scanners became available (Nutt 2002).

Energy-dependent transmembrane transport proteins (GLUT) pump glucose into cells (Fig. 3). These GLUT receptors are over-expressed on the surface of malignant cells in proportion to the rate of increased glucose metabolism. GLUT-1 is hypoxia responsive, insulin independent and the most common on cancer cells. FDG uptake in tumor cells requires a sufficient blood supply for nutrients to reach the cell. The number of viable tumor cells within a lesion determines the intensity of FDG uptake. Hypoxia-inducible factor-1-alfa up-regulates GLUT-1 by increasing tumoral FDG uptake. Rapid cell proliferation in tumors, evident by the high mitotic rate, also increases glucose utilization (Avril et al. 2001; Mochizuki et al. 2001; Bos et al. 2002).

Tumor cells have increased intracellular hexokinase levels, which phosphorylate glucose and FDG, trapping them within the cell (Smith 2000). FDG is phosphorylated by hexokinase into FDG-6-phosphate. Phosphorylated glucose rapidly undergoes glycolysis but the presence of ^{18}F on FDG-6-phosphate blocks binding of enzymes leading to glycolytic pathways. Unlike normal cells, Tumor cells show reduced levels of glucose-6-phosphatase, the enzyme that dephosphorylates D-glucose or FDG-6-phosphate, aiding accumulation of intracellular FDG. FDG accumulation in malignant cells is generally proportional to the glycolytic rate of malignant cells, which allows their detection with PET FDG imaging (Coleman 1999; Delbeke 1999; Ak et al. 2000).

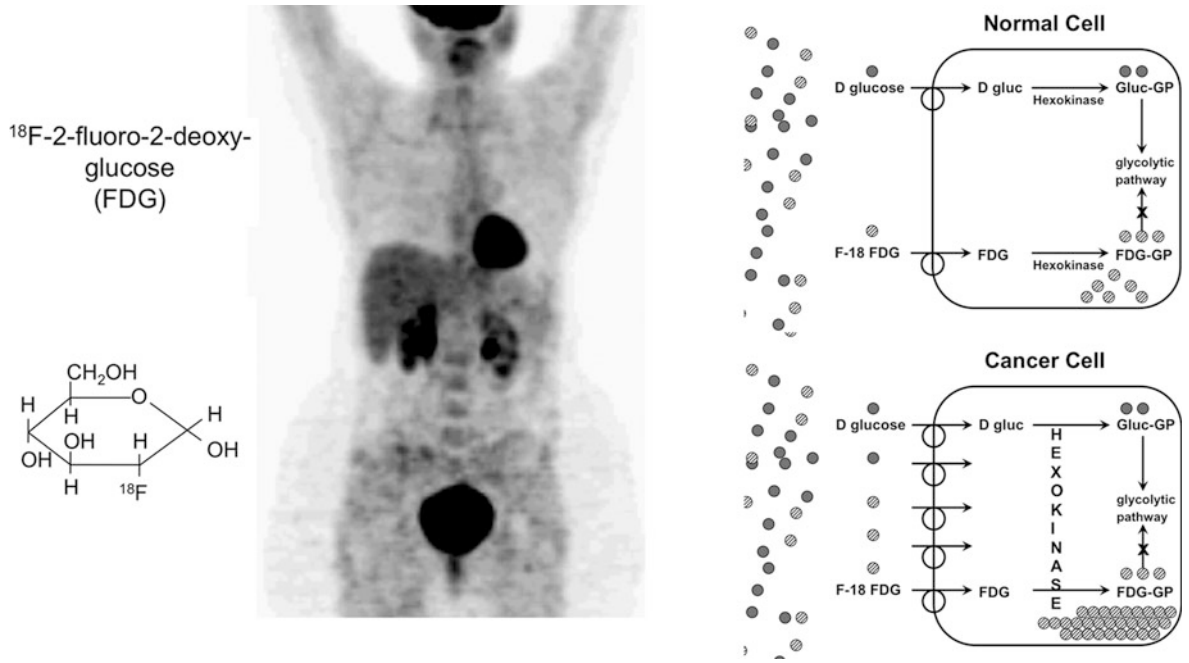

Fig. 3 ^{18}F-2-fluoro-2-deoxy-glucose (FDG) is a glucose analogue, which differs from D-glucose by the ^{18}F on the 2-carbon. Glucose and FDG are pumped into cells via the GLUT transporters on the plasma membranes. Once inside the cell, both glucose and FDG are immediately phosphorylated under the control of hexokinase. Glucose-6-phosphate can enter glycolytic pathways but the FDG-6-phosphate does not degrade because the enzyme-binding site is blocked by the ^{18}F. FDG accumulates within cancer cells in proportion to their accelerated glycolytic rate

Unfortunately, FDG is not a cancer-specific agent and accumulates avidly in inflammatory and infectious diseases, especially sarcoidosis, tuberculosis, fungal infection, and pneumonia. The increased FDG uptake is due to a marked increase in the glycolytic rate when leukocytes are activated. The increased expression of GLUT receptors and elevated hexokinase activity in activated leukocytes is very similar to tumor cells (Zhao et al. 2001; Higashi et al. 2002).

Glucose and FDG are freely filtered by the glomerulus. Glucose is then reabsorbed in the proximal convoluted tubule. The glucose transporters in the proximal convoluted tubule (SGLT1 and 2) have a limited affinity for FDG because of the ^{18}F on the 2-carbon. Only about half of the filtered FDG undergoes reuptake in the nephron. The FDG excreted in the urine leads to intense activity within the urinary system, which is normal. This normal urinary excretion of FDG clears the background activity and is beneficial for imaging. Rapid urinary excretion allows earlier imaging and lower plasma levels of FDG diminish the radiation dose to the patient (Gatley 2003).

4.1.2 ^{18}F-Sodium Fluoride

^{18}F-Sodium Fluoride (NaF) is a bone-imaging agent first introduced in 1962 and used with early gamma cameras (Blau et al.1962). NaF was the first FDA approved radiopharmaceutical. ^{18}F-NaF has a biodistribution similar to ^{99m}Tc-polyphosphonates, but with less protein binding. Following intravenous administration, NaF is rapidly removed from the plasma and either bound to bone or excreted by the kidneys. At 60 min only 10 % of the injected dose remains in the plasma. The fluoride ion is exchanged for a hydroxyl group on the hydroxyapatite crystal to form fluorapatite and is incorporated into the bone matrix. Fluoride is firmly attached at sites of osteoblastic activity and remains in the bone. NaF uptake has twice the target-to-background ratio of Tc-99m-MDP and accumulation is higher at sites of new bone formation due to the greater availability of binding

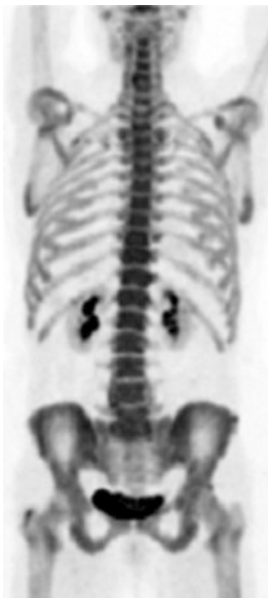

Fig. 4 ^{18}F-Sodium Fluoride (NaF) is a PET bone tracer used for evaluating osseous metastasis. NaF PET/CT is an extremely sensitive method for detecting bony metastases in patients with known malignancy. NaF normally accumulates in the bones and areas of active soft tissue calcification with renal excretion into the bladder

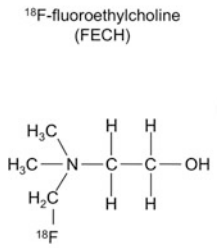

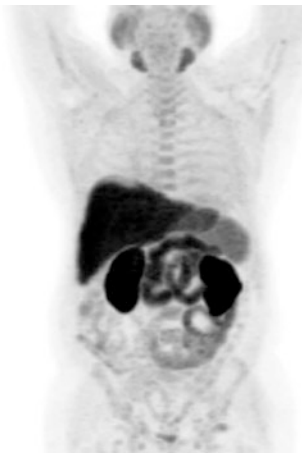

Fig. 5 ^{18}F-fluoroethylcholine (FECH) is a hypoxia tracer used for evaluating rapidly growing tumors. FECH PET/CT is extremely useful in restaging prostate cancer patients with biochemical recurrence. FECH normally accumulates in the salivary glands, pancreas, liver and intestines with renal excretion into the bladder

sites and regional hyperemia (Schiepers et al. 1997; Blake et al. 2001; Even-Sapir et al. 2004, 2006; Even-Sapir 2005) (Fig. 4).

NaF PET is very sensitive for the detection of both lytic and sclerotic bone lesions and combining it with CT increases specificity. NaF PET has a spatial resolution of 4–6 mm versus 10–15 mm for Tc-MDP imaging. NaF PET/CT has been shown to be more sensitive for detecting skeletal metastases than planar or SPECT Tc-99m-MDP skeletal imaging. Benign bone lesions like fractures, Paget disease, enchondroma, and osteoid osteomas also demonstrate increased NaF uptake. NaF PET/CT detects skeletal metastases from tumors that are typically sclerotic or have low FDG activity. FDG PET/CT is more likely to detect bone marrow metastases or small osteolytic lesions (Schirrmeister et al. 2001; Hetzel et al. 2003; Even-Sapir et al. 2004, 2006; Even-Sapir 2005).

4.2 Non-FDA Approved

The sensitivity and specificity of FDG are not optimal in all cancer types. FDG PET/CT images can not adequately differentiate between post-therapy inflammation and residual tumor, poor uptake in slow-growing tumors, and high uptake in normal cells such as the brain, which obscure tumor deposits. In the last decade, research has focused on new PET radiopharmaceuticals directed at a wide range of molecular targets including membrane synthesis, hypoxia, protein synthesis and DNA replication.

4.2.1 Membrane Synthesis

Phosphatidylcholine is an essential element of phospholipids of the cell membrane. Choline is its precursor. Choline enters most cells using specific energy-independent cell membrane transporters. Upon entering the cell, choline is phosphorylated in a reaction catalyzed by the enzyme choline kinase. The malignant transformation of cells elevates levels of choline kinase activity and phosphatidylcholine production (Howard and Howard 1975; Jackowski 1994). PET imaging with ^{11}C-choline was first evaluated in brain tumors because the normal brain has no significant phospholipid metabolism. (Hara et al. 1997) In prostate cancer ^{11}C-choline PET/CT is superior to FDG PET and conventional imaging for identifying nodal and bony metastases in patients with increasing PSA levels. (Roivainen et al. 2000; Picchio et al. 2003) The advantages of ^{11}C-choline PET imaging were apparent after initial studies, but ^{11}C-compunds have a significant logistical limitation–their half-life is only 20.4 min. Methods to label choline with fluorine-18 have been established: ^{18}F-fluoroethylcholine (FECH) is phosphorylated in vivo by choline kinase. (DeGrado et al. 2001; Hara et al. 2002) FECH (Fig. 5) is now

distributed widely for PET/CT imaging in Europe where it is used primarily for imaging prostate cancer. FECH is also useful in PET imaging of hepatocellular carcinoma and primary and metastatic brain tumors (Hara et al. 1997; Mertens et al. 2010).

4.2.2 Hypoxia

^{18}F-Fluoromisonidazole (FMISO) is a tracer used for evaluating tumor hypoxia. Hypoxia occurs in rapidly growing tumors as their need for oxygen exceeds the supply available from blood and tissue diffusion. The anoxic center of tumors typically undergoes cell death and necrosis (Fig. 6). In the borderline zones of the tumor, hypoxia inhibits cell growth and division but often leads to adaptive changes as the tumor cells struggle to survive in the harsh environment (Vaupel et al. 1992). Tumor hypoxia is a key factor in tumor progression and therapy resistance (Lee and Scott 2007). FMISO (Fig. 6) enters cells by passive diffusion and under hypoxic conditions forms a charged molecule, which binds to cellular macromolecules. FMISO is not retained in necrosis (Rasey et al. 1987; Foo et al. 2004). PET/CT with FMISO is able to assess the evolving hypoxia level in tumors during radiotherapy. Hypoxic cells are less sensitive to the cytotoxic effects of ionizing radiation than well-oxygenated cells (Koh et al. 1995). Studies in sarcoma and head and neck cancer have demonstrated a correlation of FMISO uptake with poor outcomes for radiation and chemotherapy. (Hicks et al. 2005; Rajendran et al. 2006) Other hypoxia agents include: ^{18}F-fluoroerythronitroimidazole, ^{18}F-fluoroetanidazole, and ^{62}Cu-diacetyl-bis(N (4)-methylthiosemicarbazone (^{62}-Cu-ATSM) (Beck et al. 2007; Mees et al. 2009).

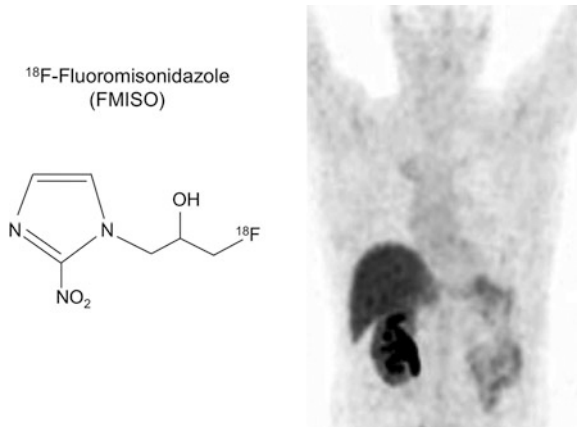

Fig. 6 ^{18}F-Fluoromisonidazole (FMISO) is a hypoxia tracer used for evaluating rapidly growing tumors. FMISO PET/CT is extremely useful in head and neck cancer patients treated with radiotherapy. FMISO normally accumulates in the liver with renal excretion into the bladder

4.2.3 Protein Synthesis

^{11}C-methionine is an amino acid that has been widely studied as a substrate for protein synthesis. Amino acids can freely diffuse into the cells, but the bulk of their transport depends on membrane glycoprotein transport. These transport systems in tumor cells can be energy-dependent, like glucose, or energy-independent. Amino acids are pumped into tumor cells in proportion to their metabolic activity. Malignant transformation drives the use of amino acids for protein synthesis as well as energy production.

Protein synthesis accelerates in proportion to the tumor mass and growth. C-methionone does not accumulate in normal brain tissue but over expressed amino acid transporters in gliomas allow visualization PET/CT. ^{11}C-methionine brain PET is useful for detection of primary tumors, evaluating suspected recurrence, predicting histopathologic grade, radiosensitivity and prognosis, guiding stereotactic brain biopsy, planning radiotherapy and assessing treatment response. (Kaschten et al. 1998; Nuutinen et al. 2000; Ribom et al. 2002; Jacobs et al. 2005; Ceyssens et al. 2006; Galldiks et al. 2006) ^{11}C-methionine PET/CT can also be used to measure increased protein synthesis in lung cancer and breast cancer (Buck et al. 2003).

3,4-Dihydroxy-^{18}F-6-fluoro-L-phenylalanine (FDOPA) was initially developed to examine the transport of a dopamine precursor in Parkinson's disease (Luxen et al. 1992). FDOPA Fig. 7 which enters the brain via a neutral amino acid carrier, is similar structurally to tyrosine but cannot be used in protein synthesis (Fig. 7). These amino acid carriers are commonly over-expressed on the plasma membranes of melanoma cells. FDOPA is extremely useful in staging and restaging of medullary thyroid carcinoma, gastrointestinal cancers, pheochromocytomas and other neuroendocrine tumors (Hoegerle et al. 1999, 2001a, b, 2002; Becherer et al. 2004). FDOPA PET/CT has greater diagnostic accuracy for detecting serotonin-expressing tumors than 111In-Octreotide SPECT or FDG PET/CT (Hoegerle et al. 2001a, b; Ilias et al. 2008). Other radiolabeled amino

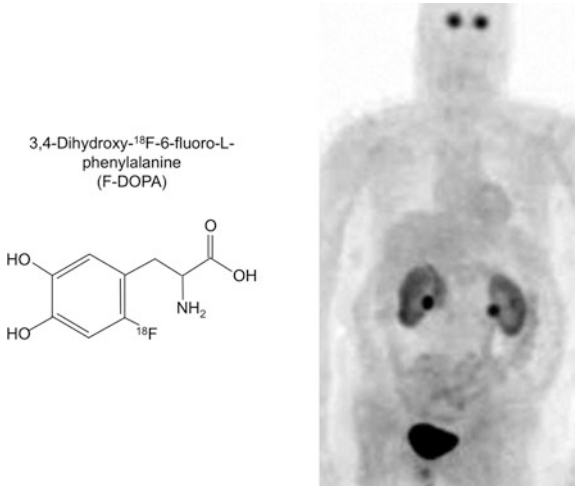

Fig. 7 3,4-Dihydroxy-^{18}F-6-fluoro-L-phenylalanine (FDOPA) is similar structurally to tyrosine and is pumped into cells by the neutral amino acid carrier FDOPA PET/CT is extremely useful in staging and restaging of neuroendocrine tumors. F-DOPA normally accumulates in the basal ganglia and liver with renal excretion into the bladder

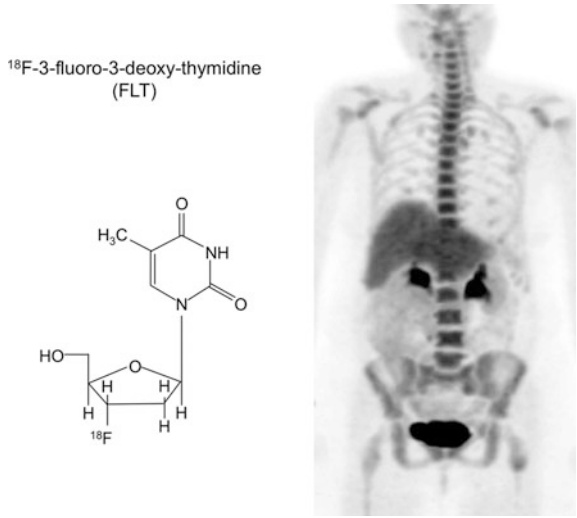

Fig. 8 ^{18}F-3-fluoro-3-deoxy-thymidine (FLT) is a radiolabeled thymidine analog, which is an indirect measure of DNA proliferation. FLT PET/CT is an imaging biomarker for early therapy assessment. FLT normally accumulates in the liver and bone marrow with renal excretion into the bladder

acid analogs include ^{18}F-L-tyrosine and ^{18}F-fluoro-cyclo-butane-1-carboxylic acid (FACBC) (Vallabhajosula 2007; Schuster et al. 2007).

4.2.4 DNA Replication

^{18}F-3-fluoro-3-deoxy-thymidine (FLT) is a pyrimidine analogue used to measure tumor cell proliferation (Fig. 8). Increased mitotic rate, cell multiplication and lack of differentiation are characteristics of the tumors. The accelerated growth of malignant tissue is the best measure of DNA replication. FLT is actively transported into the cell and phosphorylated similarly to thymidine (Sherley and Kelly 1988). FLT is trapped in the cell in proportion to the amount of DNA and RNA synthesis (Shields et al. 1996, 1998). There is a strong correlation between FLT uptake and the proliferation rate as determined by the Ki-67 index in lung, colorectal and breast cancer, melanoma, soft tissue sarcoma and brain tumors. (Vesselle et al. 2002; Francis et al. 2003; Cobben et al. 2003, 2004; Smyczek-Gargya et al. 2004; Chen et al. 2005) FLT uptake can differentiate between benign and malignant tissues and helps with tumor grading. PET/CT with FLT is useful for assessing tumor aggressiveness and early prediction of treatment response. FLT uptake does not increase with infection or inflammation like FDG. FLT, as a proliferative marker, is less affected by radiation inflammation and can detect response as early as 1 week after treatment. FLT PET/CT has a higher specificity for early therapy assessment than FDG PET/CT (Shields 2003). FLT offers more in vivo utility than FDG for evaluating patient response to novel therapies and to predict patient outcomes. Other proliferative tracers include ^{18}F-fluorouridine and ^{18}F-FMAU (Vallabhasojula 2007; Bading et al. 2008).

References

Ak I, Stokkel MP, Pauwels EK (2000) Positron emission tomography with 2-[18F]fluoro-2-deoxy-D-glucose in oncology. Part II. The clinical value in detecting and staging primary tumors. J Cancer Res Clin Oncol 126:560–574

Avril N, Menzel M, Dose J, Schelling M, Weber W, Jänicke F, Nathrath W, Schwaiger M (2001) Glucose metabolism of breast cancer assessed by 18F-FDG PET: histologic and immunohistochemical tissue analysis. J Nucl Med 42(1):9–16

Bading JR, Shields AF (2008) Imaging of cell proliferation: status and prospects. J Nucl Med 49(2):648-805

Becherer A, Szabo M, Karanikas G et al (2004) Imaging of advanced neuroendocrine tumors with [18]F-FDOPA PET. J Nucl Med 45:1161–1167

Beck R, Roper B, Carlsen JM et al (2007) Pretreatment 18F-FAZA PET predicts success of hypoxia-directed radiochemotherapy using tirapazamine. J Nucl Med 48:973–980

Blake GM, Park-Holohan SJ, Cook GJ et al (2001) Quantitative studies of bone with the use of ^{18}F-fluoride and ^{99m}Tc-methylene diphosphonate. Semin Nucl Med 31:28–49

Blau M, Nagler W, Bender MA (1962) A new isotope for bone scanning. J Nucl Med 3:332–334

Bos R, van Der Hoeven JJ, van Der Wall E, van Der Groep P, van Diest PJ, Comans EF, Joshi U, Semenza GL, Hoekstra OS, Lammertsma AA, Molthoff CF (2002) Biologic correlates of (18)fluorodeoxyglucose uptake in human breast cancer measured by positron emission tomography. J Clin Oncol 20(2):379–387

Breeman WAP, Verbruggen AM (2007) The 68 Ge/68 Ga generator has high potential, but when can we use 68 Ga-labeled tracers in clinical routine? Eur J Nucl Med Mol Imaging 34:978–981

Buck AK, Halter G, Schirrmeister H et al (2003) Imaging of proliferation in lung tumors with PET: 18FLT versus 18FDG. J Nucl Med 44:1426–1431

Carolan P, Hunt C, McConnell D et al (2012) Radiation exposure reduction to PET technologists with the use of an automated dosage delivery system. J Nucl Med 53:2185

Ceyssens S, Van Laere K, de Groot T et al (2006) [11C]methionine PET, histopathology, and survival in primary brain tumors and recurrence. AJNR 27:1432–1437

Chen W, Cloughesy T, Kamdar N et al (2005) Imaging proliferation in brain tumors with 18-FLT PET: comparison with 18F-FDG. J Nucl Med 46:945–952

Cobben DC, Elsinga PH, Suurmeijer AJ et al (2004) Detection and grading of soft tissue sarcomas of the extremities with 18F–3-fluoro-3-deoxy-l-thymidine. Clin Cancer Res 10:1685–1690

Cobben DC, Jager PL, Elsinga PH et al (2003) 18F–3-fluoro-3-deoxy-l-thymidine: a new tracer or staging of metastatic melanoma? J Nucl Med 44:1927–1932

Coleman RE (1999) PET in lung cancer. J Nucl Med 40(5):814–820

DeGrado TR, Coleman RE, Wang S et al (2001) Synthesis and evaluation of 18F labeled choline as an oncologic tracer for positron emission tomography: initial findings in prostate cancer. Cancer Res 61:110–117

Delbeke D (1999) Oncological applications of FDG PET imaging. J Nucl Med 40(10):1706–1715

Even-Sapir E, Metser U, Flusser G et al (2004) Assessment of malignant skeletal disease: initial experience with 18F–fluoride PET/CT and comparison between 18F–fluoride PET and 18F–fluoride PET/CT. J Nucl Med 45:272–278

Even-Sapir E, Metser U, Mishani E et al (2006) The detection of bone metastases in patient with high-risk prostate cancer: 99mTc-MDP planar bone scintigraphy, single- and -field-of view SPECT, 18F–fluoride PET, and 18F–fluoride PET/CT. J Nucl Med 47:287–297

Even-Sapir E (2005) Imaging of malignant bone involvement by morphologic, scintigraphic, and hybrid modalities. J Nucl Med 46:1356–1367

Foo SS, Abbott DF, Lawrentschuk N et al (2004) Functional imaging of intra-tumoral hypoxia. Mol Imaging Biol 6:291–305

Francis DL, Visvikis D, Costa DC et al (2003) Potential impact of [18F]-3-fluoro-3-deoxy-thymidine versus [18F]-fluoro-2-deoxy-D-glucose in positron emission tomography for colorectal cancer. Eur J Nucl Med Mol Imaging 30:988–994

Galldiks N, Kracht LW, Burghaus L et al (2006) Use of 11Cmethionine PET to monitor the effects of temozolomide chemotherapy in malignant gliomas. Eur J Nucl Med Mol Imaging 33:516–524

Gatley SJ (2003) Labeled glucose analogs in the genomic era. J Nucl Med 44(7):1082–1086

Hara T, Kosaka N, Kishi H (2002) Development of [18F]-Fluoroethylcholine for cancer imaging with PET: synthesis, biochemistry, and prostate cancer imaging. J Nucl Med 43:187–199

Hara T, Kosaka N, Shinoura N et al (1997) PET imaging of brain tumor with [methyl-11C] choline. J Nucl Med 38:842–847

Hetzel M, Arslandemir C, Konig HH et al (2003) F-18 NaF PET for detection of bone metastases in lung cancer: accuracy, cost-effectiveness and impact on patient management. J Bone Miner Res 18:2206–2214

Hicks RJ, Rischin D, Fisher R et al (2005) Utility of FMISO PET in advanced head and neck cancer treated with chemoradiation incorporating a hypoxia-targeting chemotherapy agent. Eur J Nucl Med Mol Imaging 32:1384–1391

Higashi T, Saga T, Nakamoto Y, Ishimori T, Mamede MH, Wada M, Doi R, Hosotani R, Imamura M, Konishi J (2002) Relationship between retention index in dual-phase (18)F-FDG PET, and hexokinase-II and glucose transporter-1 expression in pancreatic cancer. J Nucl Med 43(2):173–180

Hoegerle S, Altehoefer C, Ghanem N et al (2001a) 18F-DOPA positron emission tomography for tumor detection in patients with medullary thyroid carcinoma and elevated calcitonin levels. Eur J Nucl Med 28:64–71

Hoegerle S, Altehoefer C, Ghanem N, Koehler G, Waller CF, Scheruebl H, Moser E, Nitzsche E (2001b) Whole-body 18F dopa PET for detection of gastrointestinal carcinoid tumors. Radiology 220(2):373–380

Hoegerle S, Nitzsche E, Altehoefer C et al (2002) Pheochromocytomas: detection with 18F DOPA whole body PET—initial results. Radiology 222:507–512

Hoegerle S, Schneider B, Kraft A, Moser E, Nitzsche EU (1999) Imaging of a metastatic gastrointestinal carcinoid by F-18-DOPA positron emission tomography. Nuklearmedizin 38:127–130

Howard BV, Howard WJ (1975) Lipids in normal and tumor cells in culture. Prog Biochem Pharmacol 10:135–166

Ido T, Wan CN, Casella JS et al (1978) Labeled 2-deoxy-D-glucose analogs: 18F labeled 2-deoxy-2-fluoro-D-glucose, 2-deoxy-2-fluoro-D-mannose and 14C–2-deoxy-2-fluoro-D-glucose. J Label Compd Radiopharmacol 14:175–183

Ilias I, Chen CC, Carrasquillo JA et al (2008) Comparison of 6-[18F]-fluorodopamine positron emission tomography to [123I]-metaiodobenzylguanidine and [111In]-pentetreotide scintigraphy in the localization of non-metastatic and metastatic pheochromocytoma. J Nucl Med 49:1613–1619

Jackowski S (1994) Coordination of membrane phospholipid synthesis with the cell cycle. J Biol Chem 269: 3858–3867

Jacobs AH, Thomas A, Kracht LW et al (2005) 18F-fluoro-l-thymidine and 11C-Methylmetionine as markers of increased transport and proliferation in brain tumors. J Nucl Med 46:1948–1958

Kaschten B, Stevenaert A, Sadzot B et al (1998) Preoperative evaluation of 54 gliomas by PET with fluorine-18-fluorodeoxyglucose and/or carbon-11-methionine. J Nucl Med 39:778–785

Koh WJ, Bergman KS, Rasey JS et al (1995) Evaluation of oxygenation status during fractionated radiotherapy in human non-small cell lung cancers using [F-18]fluoromisonidazole positron emission tomography. Int J Radiat Oncol Biol Phys 33:391–398

Laszlo J, Humphreys SR, Goldin A (1960) Effects of glucose analogues (2-deoxy-D-glucose, 2-deoxy-D-galactose) on experimental tumors. J Natl Cancer Inst 24:267–281

Lee ST, Scott AM (2007) Hypoxia positron emission tomography imaging with 18F-fluoromisonidazole. Semin Nucl Med 37:451–461

Luxen A, Guillaume M, Melega WP et al (1992) Production of 6-[18F]fluoro-L-dopa and its metabolism in vivo—a critical review. Int J Radiat Appl Instrum B 19:149–158

McCarthy TJ, Welch MJ (1998) The state of positron emitting radionuclide production in 1997. Semin Nucl Med 28(3): 235–46

Mees G, Dierckx R, Vangestel C et al (2009) Molecular imaging of hypoxia with radiolabeled agents. Eur J Nucl Med Mol Imaging 36:1674–1686

Mertens K, Slaets D, Lambert B, Acou M, De Vos F, Goethals I (2010) PET with (18)F-labeled choline-based tracers for tumor imaging: a review of the literature. Eur J Nucl Med Mol Imaging 37(11):2188–2193

Mochizuki T, Tsukamoto E, Kuge Y, Kanegae K, Zhao S, Hikosaka K, Hosokawa M, Kohanawa M, Tamaki N (2001) FDG uptake and glucose transporter subtype expressions in experimental tumor and inflammation models. J Nucl Med 42(10):1551–1555

Nutt R (2002) The history of positron emission tomography (PET). Mol Imaging Biol 4:11–26

Nuutinen J, Sonninen P, Lehikoinen P et al (2000) Radiotherapy treatment planning and long-term follow-up with [(11)C] methionine PET in patients with low-grade astrocytoma. Int J Radiat Oncol Biol Phys 48:43–52

Pacák J, Cerny M (2002) History of the First Synthesis of 2-Deoxy-2-Fluoro-D-Glucose the Unlabeled Forerunner of 2-Deoxy-2-[18F]Fluoro-D-Glucose. Mol Imaging Biol 4:353–354

Picchio M, Messa C, Landoni C et al (2003) Value of [11C]choline positron emission tomography for re-staging prostate cancer: a comparison with [18F] fluorodeoxyglucose-positron emission tomography. J Urol 169:1337–1340

Rajendran JG, Schwartz DL, O'Sullivan J et al (2006) Tumor hypoxia imaging with [F-18] fluoromisonidazole positron emission tomography in head and neck cancer. Clin Cancer Res 12:5435–5441

Rasey JS, Grunbaum Z, Magee S et al (1987) Characterization of radiolabeled fluoromisonidazole as a probe for hypoxic cells. Radiat Res 111:292–304

Ribom D, Engler H, Blomquist E, Smits A (2002) Potential significance of (11)C-methionine PET as marker for the radiosensitivity of low-grade gliomas. Eur J Nucl Med Mol Imaging 29:632–640

Rice SL, Roney CA, Daumar P, Lewis JS (2011) The next generation of positron emission tomography radiopharmaceuticals in oncology. Semin Nucl Med 41(4):265–282

Roivainen A, Forsback S, Grönroos T et al (2000) Blood metabolism of [methyl-11C]choline; implications for in vivo imaging with positron emission tomography. Eur J Nucl Med 27:25–32

Rufini V, Calcagni ML, Baum RP (2007) Imaging of neuroendocrine tumors. Semin Nucl Med 36:228–247

Schiepers C, Nuytes J, Bormans G et al (1997) Fluoride kinetics of the axial skeleton measured in vivo with fluorine-18-fluoride PET. J Nucl Med 38:1970–1976

Schirrmeister H, Glatting G, Hetzel J et al (2001) Prospective evaluation of clinical value of planar bone scans, SPECT, and18F-labeled NaF PET in newly diagnosed lung cancer. J Nucl Med 42:1800–1804

Schlyer DJ (2004) PET tracers and radiochemistry. Ann Acad Med Singapore 33:146–154

Schuster DM, John R, Votaw JR et al (2007) Initial experience with the radiotracer anti-1-amino-3-18F-fluorocyclobutane-1-carboxylic acid with PET/CT in prostate carcinoma. J Nucl Med 48:56–63

Shaiju VS, Sharma SD, Kumar R, Sarin B (2009) Target foil rupture scenario and provision for handling different models of medical cyclotrons used in India. J Med Phys 34(3):161–166

Sharma S, Krause G, Ebadi M (2006) Radiation safety and quality control in the cyclotron laboratory. Radiat Prot Dosimetry 118:431–439

Sherley JL, Kelly TJ (1988) Regulation of human thymidine kinase during the cell cycle. J Biol Chem 263:8350–8358

Shields AF (2003) PET imaging with 18F-FLT and thymidine analogs: promise and pitfalls. J Nucl Med 44:1432–1434

Shields AF, Grierson JR, Kozawa SM et al (1996) Development of labeled thymidine analogs for imaging tumor proliferation. Nucl Med Biol 23:17–22

Shields AF, Grierson JR, Dohmen BM et al (1998) Imaging proliferation in vivo with [F-18]FLT and positron emission tomography. Nat Med 4:1334–1336

Smith TA (2000) Mammalian hexokinases and their abnormal expression in cancer. Br J Biomed Sci 57:170–178

Smyczek-Gargya B, Fersis N, Dittmann H et al (2004) PET with [18F]fluorothymidine for imaging of primary breast cancer: a pilot study. Eur J Nucl Med Mol Imaging 31:720–724

Vallabhajosula S, Solnes L, Vallabhajosula B (2011) A broad overview of positron emission tomography radiopharmaceuticals and clinical applications: what is new? Semin Nucl Med 41(4):246–264

Vallabhajosula S (2007) (18)F-labeled positron emission tomographic radiopharmaceuticals in oncology: an overview of radiochemistry and mechanisms of tumor localization. Semin Nucl Med 37(6):400–419

Vaupel P, Schlenger K, Hoeckel M (1992) Blood flow and tissue oxygenation of human tumors: an update. Adv Exp Med Biol 317:139–151

Vesselle H, Grierson J, Muzi M et al (2002) In vivo validation of 3′deoxy-3′-[(18)F]fluorothymidine ([(18)F]FLT) as a proliferation imaging tracer in humans: correlation of [(18)F]FLT uptake by positron emission tomography with

Ki-67 immunohistochemistry and flow cytometry in human lung tumors. Clin Cancer Res 8:3315–3323

Warburg O (1956) On the origin of cancer cells. Science 123:309–314

Williams HA, Robinson S, Julyan P et al (2005) A comparison of PET imaging characteristics of various copper radioisotopes. Eur J Nucl Med Mol Imaging 32:1473–1480

Zhao S, Kuge Y, Tsukamoto E, Mochizuki T, Kato T, Hikosaka K, Hosokawa M, Kohanawa M, Tamaki N (2001) Effects of insulin and glucose loading on FDG uptake in experimental malignant tumors and inflammatory lesions. Eur J Nucl Med 28(6):730–735

Zhernosekov KP, Filosofov DV, Baum RP et al (2007) Processing of generator-produced 68 Ga for medical application. J Nucl Med 48:1741–1748

Zweit J, Goodall R, Cox M, Babich JW, Potter GA, Sharma HL, Ott RJ (1992) Development of a high performance zinc-62/copper-62 radionuclide generator for positron emission tomography. Eur J Nucl Med 19(6):418–425